New Electrophilic Iridium(I) Complexes: H−H and C−H Bond Heterolysis by $[(dfepe)Ir(\mu\text{-}X)]_2$ (X = O_2CCF_3, OTf)

R. Chris Schnabel and Dean M. Roddick*

Department of Chemistry, Box 3838, University of Wyoming, Laramie, Wyoming 82071

Received March 22, 1996[⊗]

New electrophilic dimeric iridium(I) complexes $[(dfepe)Ir(\mu\text{-}X)]_2$ (dfepe = $(C_2F_5)_2PCH_2CH_2P(C_2F_5)_2$; X = O_2CCF_3, OTf) have been prepared and their reactions with H_2 and cyclopentane examined. Treatment of $[(cod)Ir(O_2CCF_3)]_2$ with dfepe produced an ionic product $[(dfepe)Ir(cod)]^+[(dfepe)Ir(O_2CCF_3)_2]^-$ (**1**), which in refluxing benzene rearranged with loss of cyclooctadiene to form $[(dfepe)Ir(\mu\text{-}O_2CCF_3)]_2$ (**2**). The corresponding reaction of $[(cod)Rh(O_2CCF_3)]_2$ with dfepe yielded $[(dfepe)Rh(\mu\text{-}O_2CCF_3)]_2$ (**3**) directly. X-ray diffraction analysis of **2** revealed a hinged dimeric geometry with an unusually large interplanar angle of 82.7° defined by the two 4-coordinate metal centers (Ir(1)−Ir(2) = 4.307 Å). The triflate-bridged analogue of **2** was prepared via an indirect route: addition of 1 equiv of triflic acid to $(dfepe)Ir(\eta^3\text{-}C_3H_5)$ yielded the allyl hydride complex $(dfepe)Ir(\eta^3\text{-}C_3H_5)(H)(OTf)$ (**4**), which eliminated propylene in refluxing heptane to quantitatively afford $[(dfepe)Ir(\mu\text{-}O_3SCF_3)]_2$ (**5**). The structure of **4** was confirmed by X-ray diffraction. In contrast to $[(dfepe)Ir(\mu\text{-}Cl)]_2$, the acetate- and triflate-bridged analogues **2** and **5** are reactive toward both H_2 and alkane C−H bonds. Treatment of **2** with H_2 (20 °C) or cyclopentane (150 °C) cleanly afforded $(dfepe)_2Ir_2(\mu\text{-}H)_2(H)(\mu\text{-}O_2CCF_3)$ (**6**) and CpIr(dfepe), respectively. Surprisingly, the corresponding reactions of **5** are significantly slower, suggesting that the concomitant release of the stronger acid CF_3SO_3H may inhibit these heterolysis reactions.

Introduction

The development of robust homogeneous hydrocarbon functionalization catalysts remains a challenging goal.[1] Although systems based on reactive electron-rich $(R_3P)_2MX$ (M = Rh, Ir; X = Cl) intermediates have been reported which promote hydrogen transfer and hydrocarbon carbonylation, these systems are generally incompatible with oxidative environments.[2] Heterolytic hydrocarbon activation systems based on simple metal salts in acidic media have received renewed attention, but comparatively little is known about the mechanistic details of these systems.[3]

Recently we reported the synthesis and reactivity properties of the (perfluoroalkyl)phosphine dimers $[(dfepe)M(\mu\text{-}Cl)]_2$ (dfepe = $(C_2F_5)_2PCH_2CH_2P(C_2F_5)_2$; M = Rh, Ir).[4] While these electron-poor compounds do exhibit exceptional air and thermal stability, they are unreactive toward H−H or aliphatic C−H bonds. This observed lack of reactivity may be ascribed in part to an intrinsic lowered reactivity of $(dfepe)M^I$ metal centers relative to donor phosphine analogues toward simple oxidative addition; however, an additional factor to consider is the inaccessibility of a more reactive 14-electron (dfepe)MCl intermediate via chloride bridge dissociation. We have begun a systematic study of bridging ligand effects in order to assess this latter possibility, and herein describe the synthesis and structure of trifluoroacetate- and triflate-bridged complexes, $[(dfepe)M(\mu\text{-}O_2CCF_3)]_2$ and $[(dfepe)Ir(\mu\text{-}O_3SCF_3)]_2$, and the enhanced reactivity of these new iridium dimers toward dihydrogen and hydrocarbon C−H bonds.

Results and Discussion

Synthesis and Structure of $[(dfepe)M(\mu\text{-}O_2CCF_3)]_2$ (M = Rh, Ir) Complexes. Crabtree has reported the synthesis of $(R_3P)_2Ir(O_2CCF_3)(H)_2$ complexes from the in situ treatment of $[(cod)Ir(O_2CCF_3)]_2$ with the appropriate phosphine and dihydrogen.[5] When $[(cod)Ir(O_2CCF_3)]_2$ was treated with dfepe in the absence of H_2, a red crystalline solid (**1**) was obtained in high yield (Scheme 1). Warming **1** in benzene cleanly afforded the light yellow cod-free acetate dimer $[(dfepe)Ir(\mu\text{-}O_2CCF_3)]_2$ (**2**). The insolubility of **1** in nonpolar solvents and the rapid loss of cod in polar coordinating solvents limited spectroscopic characterization; however, quantification of the released cod upon solvation of **1** in acetone-d_6 by ^1H NMR and microanalytical data are consistent with the empirical formulation $(dfepe)_2Ir_2(O_2CCF_3)_2(cod)$. **1** was originally believed to be a dimeric μ-cod complex $[(dfepe)Ir(\mu\text{-}O_2CCF_3)]_2(\mu\text{-cod})$; however, solubility properties and the qualitative similarities between the UV−vis spectra of **1** and the previously reported monomeric cationic complex $[(dfepe)Ir(cod)]O_3$-

[⊗] Abstract published in *Advance ACS Abstracts,* July 15, 1996.

(1) (a) *Selective Hydrocarbon Activation*; Davies, J. A., Watson, P. L., Liebman, J. F., Greenberg, A., Eds.; VCH Publishers: New York, 1990. (b) *Activation and Functionalization of Alkanes*; Hill, C. L., Ed.; Wiley: New York, 1989. (c) Crabtree, R. H. *Chem. Rev.* **1985**, *85*, 245.

(2) (a) Tanaka, M.; Sakakura, T. *Adv. Chem. Ser.* **1992**, *No. 230*, 181. (b) Maguire, J. A.; Petrillo, A.; Goldman, A. S. *J. Am. Chem. Soc.* **1992**, *114*, 9492. (c) Aoki, T.; Crabtree, R. H. *Organometallics* **1993**, *12*, 294.

(3) (a) Periana, R. A.; Taube, D. J.; Evitt, E. R.; Loffler, D. G.; Wentrcek, P. R.; Voss, G.; Masuda, T. *Science* **1993**, *259*, 340. (b) Sen, A. *Platinum Met. Rev.* **1990**, *35*, 126. (c) Sen, A. *Acc. Chem. Res.* **1988**, *21*, 421. (d) Vargaftik, M. N.; Stolarov, I. P.; Moiseev, I. I. *J. Chem. Soc., Chem. Commun.* **1990**, 1049. (e) Labinger, J. A.; Herring, A. M.; Bercaw, J. E. *J. Am. Chem. Soc.* **1990**, *112*, 5628. (f) Shilov, A. E. *Activation of Saturated Hydrocarbons by Transition Metals;* Reidel: Dordrecht, The Netherlands, 1984; Chapter 5.

(4) Schnabel, R. C.; Roddick, D. M. *Inorg. Chem.* **1993**, *32*, 1513.

(5) Burk, M. J.; Crabtree, R. H. *J. Am. Chem. Soc.* **1987**, *109*, 8025.

S0276-7333(96)00216-6 CCC: $12.00

Scheme 1

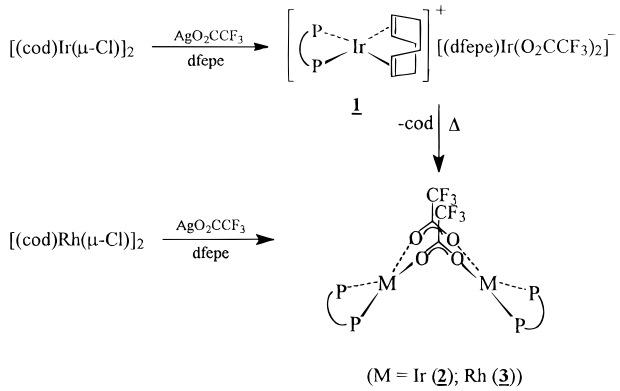

(M = Ir (**2**); Rh (**3**))

SCF_3 (see Experimental Section) suggest the ionic formulation $[(dfepe)Ir(cod)]^+[(dfepe)Ir(O_2CCF_3)_2]^-$ as a more likely alternative for **1**.[6]

Further support for acetate disproportionation is given by IR data, which exhibit a $\Delta(\nu(O_2CCF_3)_{sym} - \nu(O_2CCF_3)_{asym}) = 288$ cm^{-1} that is well within range for unidentate acetate coordination.[7] The analogous rhodium complex $[(dfepe)Rh(\mu\text{-}O_2CCF_3)]_2$ (**3**) was prepared directly from $[(cod)Rh(\mu\text{-}O_2CCF_3)]_2$ without any evidence for a stable cyclooctadiene intermediate. Infrared data are often diagnostic for carboxylate ligand coordination modes; however, $\nu(CO_2)$ data for **2** and **3** do not follow established trends.[7] In particular, although $\nu(CO_2)_{asym}$ bands are observed (**2** (CH_2Cl_2), 1674 cm^{-1}; **3**, 1682 cm^{-1}), no characteristic CF_3CO_2 $\nu(CO_2)_{sym}$ bands are seen for either **2** or **3** between 1400 and 1460 cm^{-1} either in solution or in the solid state. An acetate-bridged dimeric geometry is nevertheless indicated by ^{31}P, ^{19}F, and ^1H NMR data for complexes **2** and **3**, which both show single resonances for dfepe backbone, phosphorus, and the C_2F_5 trifluoromethyl groups. The NMR data taken together with structural data (see below) indicate that bent dimeric $[(dfepe)M(\mu\text{-}O_2CCF_3)]_2$ complexes, like previously reported $[(dfepe)M(\mu\text{-Cl})]_2$ analogues, undergo a rapid hinge inversion process on the NMR time scale. This is in contrast with the static hinged geometry reported for $[(cod)Ir(\mu\text{-}O_2CCF_3)]_2$.[8]

The dimeric geometry of **2** has been confirmed by X-ray crystallography (Figure 1). A summary of data collection parameters and selected bond distances and angles are tabulated in Tables 1 and 2, respectively. The folded dimeric square planar geometry of **2** is similar to that of $[(nbd)Rh(\mu\text{-}O_2CMe)]_2$[9,10] and also structurally-characterized isoelectronic palladium(II) and platinum(II) bridging acetate systems such as $[(Ph_3P)(Ph)Pd(\mu\text{-}O_2CMe)]_2$ and $[(en)Pt(\mu\text{-}O_2CCH_2SO_3]_2$.[11,12] A key difference, however, between **2** and related structures is a significant flattening of the dimer, as evidenced by the large interplanar angle of 82.7° defined by the two 4-coordinate metal centers (Ir(1)−Ir(2) = 4.307 Å). All other comparable structures exhibit a considerably more acute folding angle between 34 and 59° (M−M = 2.9−3.4 Å).[11−13] The observed difference is apparently steric in origin. The closest intramolecular F−F contacts for **2** occur between opposing dfepe ligand CF_3 groups (F(32)−F(17) = 2.83 Å; F(31)−F(20) = 2.87 Å). These distances are comparable to previously reported intermolecular F−F contacts, which vary between 2.73 and 2.90 Å and are within the normal van der Waals contact

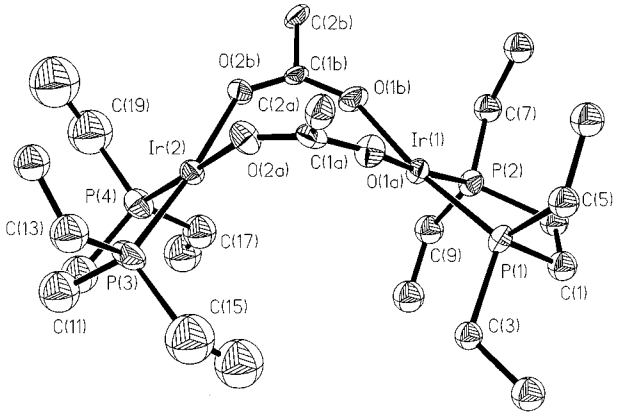

Figure 1. Molecular structure of $[(dfepe)Ir(\mu\text{-}O_2CCF_3]_2$ (**2**) with atom-labeling scheme (30% probability ellipsoids). Fluorine and hydrogen atoms have been omitted for clarity.

Table 1. Crystallographic Data for $[(dfepe)Ir(\mu\text{-}O_2CCF_3)]_2$ (2) and $(dfepe)Ir(\eta^3\text{-}C_3H_5)(H)O_3SCF_3$ (4)

	$[(dfepe)Ir(\mu\text{-}O_2CCF_3)]_2$	$(dfepe)Ir(\eta^3\text{-}C_3H_5)(H)O_3SCF_3$
	Crystal Data	
chem formula	$C_{24}H_8F_{46}Ir_2O_4P_4$	$C_{14}H_{10}F_{23}IrO_3P_2S$
fw	1742.6	949.4
cryst system	monoclinic	orthorhombic
color	orange	yellow
space group	$P2_1/n$ (No. 14)	$P2_12_12_1$ (No. 19)
size (mm)	0.46 × 0.60 × 0.64	0.20 × 0.34 × 0.46
a (Å)	17.590(5)	8.215(2)
b (Å)	13.895(3)	15.720(3)
c (Å)	19.793(5)	19.878(4)
β (deg)	111.85(2)	
V (Å^3)	4490(2)	2567.0(9)
Z	4	4
T (°C)	−100	−110
λ (Å)	0.710 73	0.710 73
D_{calc} (g cm^{-3})	2.578	2.454
μ (cm^{-1})	62.61	55.64
T(max)/T(min)	0.0405/0.0170	0.624/0.413
	Data Collection	
scan method	$2\theta/\theta$	Wyckoff
scan limits (deg)	4−45	4−55
data collcd (h,k,l)	+18,+14,±21	−10,+20,25
rflns collcd	6418	3330
indpndt rflns	5891	3330
obsd rflns	3982 ($F_o > 4\sigma(F_o)$)	2645 ($F_o > 4\sigma(F_o)$)
	Refinement[a]	
$R(F)$ (%)	6.81	5.29
R(wF) (%)	9.87	5.81
GOF	0.80	1.35
Δ/σ(max)	0.002	0.000
$\Delta(\rho)$ (e Å^{-3})	2.15	2.61
N_o/N_v	9.5	6.7

[a] $R(F_o) = \Sigma(|F_o| - |F_c|)/\Sigma|F_o|$, $R_w(F_o) = \Sigma(w^{1/2}(|F_o| - |F_c|))/\Sigma(w^{1/2}|F_o|)$, $w^{-1} = \sigma^2(F_o) + 0.0008(F_o)^2$.

(6) Schnabel, R. C.; Roddick, D. M. *Organometallics* **1993**, *12*, 704.
(7) Deacon, G. B.; Phillips, R. J. *Coord. Chem. Rev.* **1980**, *33*, 227.
(8) Feldman, J.; Calabrese, J. C. *Inorg. Chem.* **1994**, *33*, 5955.
(9) Reis, A. H.; Willi, C.; Siegel, S.; Tani, B. *Inorg. Chem.* **1979**, *18*, 1859.
(10) The crystal structure of $[(nbd)Rh(\mu\text{-}O_2CCF_3)]_2$ has been reported without metrical details: Azbel, B. I.; Gol'dshleger, N. F.; Khidekel, M. L.; Sokol, V. I.; Porai-Koshits, M. A. *J. Mol. Catal.* **1987**, *40*, 57.
(11) Hursthouse, M. B.; Sloan, O. D.; Thornton, P.; Walker, N. P. C. *Polyhedron* **1986**, *5*, 1475.
(12) Miyamoto, T. K.; Ichida, H. *Bull. Chem. Soc. Jpn.* **1991**, *64*, 1835.
(13) (a) Wong-Ng, W.; Cheng, P. T.; Kocman, V.; Luth, H.; Nyburg, S. C. *Inorg. Chem.* **1979**, *18*, 2620. (b) Gainsford, G. J.; Mason, R. *J. Organomet. Chem.* **1974**, *80*, 395. (c) Wehman, E.; van Koten, G.; Jastrzebski, J. T. B. H.; Ossor, H.; Pfeffer, M. *J. Chem. Soc., Dalton Trans.* **1988**, 2975.

Table 2. Selected Bond Lengths (Å) and Angles (deg) for [(dfepe)Ir(μ-O_2CCF_3)]$_2$ (2)

Bond Distances			
Ir(1)−P(1)	2.151(6)	Ir(1)−P(2)	2.145(6)
Ir(1)−O(1a)	2.08(1)	Ir(1)−O(1b)	2.11(2)
Ir(2)−P(3)	2.143(8)	Ir(2)−P(4)	2.129(7)
Ir(2)−O(2a)	2.08(2)	Ir(2)−O(2b)	2.10(2)
O(1a)−C(1a)	1.25(3)	O(2a)−C(1a)	1.22(3)
O(1b)−C(1b)	1.20(2)	O(2b)−C(1b)	1.21(3)
C(1a)−C(2a)	1.51(3)	C(1b)−C(2b)	1.59(4)

Bond Angles			
P(1)−Ir(1)−P(2)	84.4(2)	P(3)−Ir(2)−P(4)	84.4(3)
P(1)−Ir(1)−O(1a)	93.3(4)	P(1)−Ir(1)−O(1b)	172.0(6)
P(2)−Ir(1)−O(1a)	173.4(5)	P(2)−Ir(1)−O(1b)	91.7(5)
O(1a)−Ir(1)−O(1b)	89.8(6)	O(2a)−Ir(2)−O(2b)	87.9(7)
P(3)−Ir(2)−O(2a)	94.1(6)	P(3)−Ir(2)−O(2b)	173.8(5)
P(4)−Ir(2)−O(2a)	177.5(5)	P(4)−Ir(2)−O(2b)	93.4(5)
O(1a)−C(1a)−O(2a)	131(2)	O(1b)−C(1b)−O(2b)	135(2)

Scheme 2

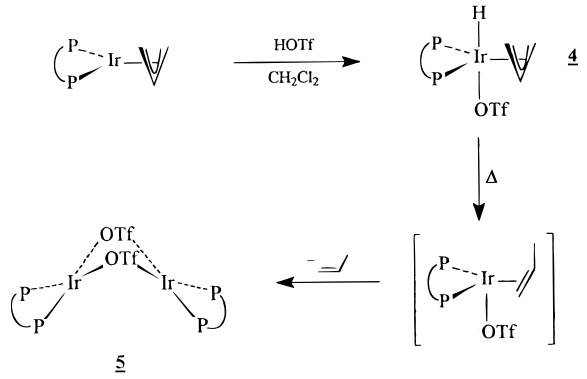

range for fluorocarbon substituents.[14] A further indication of steric interactions between the dfepe ligands is the significant displacement of phosphorus atoms P(1)−P(4) of 0.28, 0.24, 0.22, and 0.08 Å, respectively, away from planes defined by Ir(1)−O(1a)−O(1b) and Ir(2)−O(2a)−O(2b).

Synthesis of [(dfepe)Ir(μ-O_3SCF_3)]$_2$. A synthesis of the triflate-bridged dimeric complex [(dfepe)Ir(μ-O_3SCF_3)]$_2$ analogous to Scheme 1 is not possible, since the reaction of [(cod)Ir(thf)$_2$]OTf with dfepe results in solvent displacement and the preferential formation of [(dfepe)Ir(cod)]OTf.[6] Instead, an indirect route to [(dfepe)Ir(μ-O_3SCF_3)]$_2$ was developed utilizing the previously reported allyl complex, (dfepe)Ir(η^3-C_3H_5) (Scheme 2).[15] Addition of 1 equiv of triflic acid to (dfepe)Ir(η^3-C_3H_5) in dichloromethane at 20 °C resulted an immediate bleaching of the orange solution to give colorless (dfepe)Ir(η^3-C_3H_5)(H)(OTf) (**4**). Although we anticipated that the electron-poor nature of **4** would lead to rapid reductive elimination of propylene and generation of the desired triflate compound, the Ir(III) allyl hydride complex is moderately stable and was isolated in good yield from CH_2Cl_2/ether. An extension of this protonolysis procedure to the synthesis of cationic [(dfepe)Ir(η^3-C_3H_5)(H)]$^+X^-$ complexes by employing more weakly coordinating acids such as HBF_4, HPF_6, or $HBAr_4$ (Ar = 3,5-$(CF_3)_2C_6H_3$) was attempted, but no evidence for these anticipated products was obtained.[16]

Subsequent thermolysis of **4** in refluxing heptane for 24 h resulted in the clean elimination of propylene (identified by ^{1}H NMR) and afforded [(dfepe)Ir(μ-O_3SCF_3)]$_2$ (**5**) in nearly quantitative yield. Triflate infrared data for **5** ($\nu_{asym}(SO_3) = 1324$ cm^{-1}, $\nu_{sym}(SO_3) = 1019$ cm^{-1}) are essentially identical to that reported for the structurally-characterized iridium complex (dfepe)$_2$Ir$_2$(μ-H)(H)(μ-OTf) and is thus consistent with a bridged-triflate dimer formulation analogous to [(dfepe)Ir(μ-O_2CCF_3)]$_2$.[6]

Although NMR data for **4** confirm the presence of hydride (triplet, δ −30.41, $^2J_{PH} = 15$ Hz) and η^3-C_3H_5 ligands, the disposition of the hydride, triflate, and allyl ligands with respect to the dfepe chelate is not uniquely determined. To address this ambiguity the stereochemistry of **4** was determined by X-ray diffraction. Collection parameters and selected metrical data for **4** are given in Tables 1 and 3, respectively. Although the hydride was not located, its presence trans to the triflate ligand is inferred from the void space in the iridium coordination sphere opposite O(1) (Figure 2). The geometry about the iridium may be formally viewed as pseudo-octahedral, with the allyl ligand occupying two cis coordination sites. The disposition of the allyl ligand

Table 3. Selected Bond Lengths (Å) and Angles (deg) for (dfepe)Ir(η^3-C_3H_5)(H)O_3SCF_3 (4)

Bond Distances			
Ir(1)−P(1)	2.240(5)	Ir(1)−P(2)	2.242(4)
Ir(1)−C(11)	2.21(2)	Ir(1)−C(12)	2.21(2)
Ir(1)−C(13)	2.26(2)	Ir(1)−O(1)	2.28(1)
C(11)−C(12)	1.37(3)	C(12)−C(13)	1.47(3)
S(1)−O(1)	1.45(1)	S(1)−O(2)	1.41(1)
S(1)−O(3)	1.41(1)	S(1)−C(14)	1.76(2)

Bond Angles			
P(1)−Ir(1)−P(2)	85.3(2)	P(1)−Ir(1)−Ca[a]	135.8
P(2)−Ir(1)−Ca	137.3	O(1)−Ir(1)−Ca	91.6
P(1)−Ir(1)−O(1)	98.4(3)	P(2)−Ir(1)−O(1)	92.7(3)
S(1)−O(1)−Ir(1)	146.8(8)	O(1)−S(1)−O(2)	115.1(8)
O(1)−S(1)−O(3)	114.0(7)	O(2)−S(1)−O(3)	116.5(9)
O(1)−S(1)−C(14)	102.0(9)	O(2)−S(1)−C(14)	102.0(9)
O(3)−S(1)−C(14)	104.6(11)	C(11)−C(12)−C(13)	120(2)

[a] Ca = unweighted centroid of the η^3-allyl ligand.

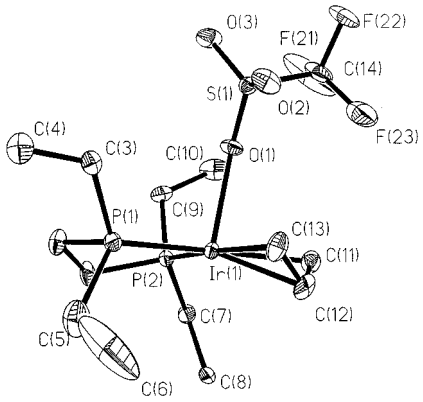

Figure 2. Molecular structure of (dfepe)Ir(η^3-C_3H_5)(H)O_3-SCF_3 (**4**) with atom-labeling scheme (30% probability ellipsoids). Fluorine and hydrogen atoms have been omitted for clarity.

(14) A survey of intermolecular fluorocarbon F−F distances in the Cambridge Crystallographic Database showed that contacts as short as 2.75 Å are not unusual: Guggenburger, L. J. *Acta Crystallogr. B* **1973**, *29*, 2110.

(15) Schnabel, R. C; Carroll, P. S.; Roddick, D. M. *Organometallics* **1996**, *15*, 655.

(16) A coordinatively unsaturated cationic Ir(III) allyl complex of this type has been reported: Howarth, O. W.; McAteer, C. H.; Moore, P.; Morris, G. E. *J. Chem. Soc., Chem. Commun.* **1981**, 506.

with respect to dfepe and the other two anionic ligands parallels the geometries reported for other $(R_3P)_2Ir(III)$ systems.[17]

Reactivity Trends of [(dfepe)Ir(μ-X)]$_2$ Complexes. The chemistry of the trifluoroacetate- and triflate-bridged dimers differs markedly from that of [(dfepe)-Ir(μ-Cl)]$_2$. Unlike [(dfepe)Ir(μ-Cl)]$_2$, which is unreactive toward dihydrogen, exposure of an acetone solution of [(dfepe)Ir(μ-O_2CCF_3)]$_2$ to *ca.* 2 atm of H_2 at ambient temperature results in the loss of 1 equiv CF_3CO_2H after 2 days and the clean formation of the unsymmetrical trihydride dimer (dfepe)$_2$Ir$_2$(μ-H)$_2$(H)(μ-O_2CCF_3) (**6**) (eq 1). Solutions of the rhodium analogue **3** under H_2 slowly darkened over the course of several hours, but no products similar to **6** were isolated.

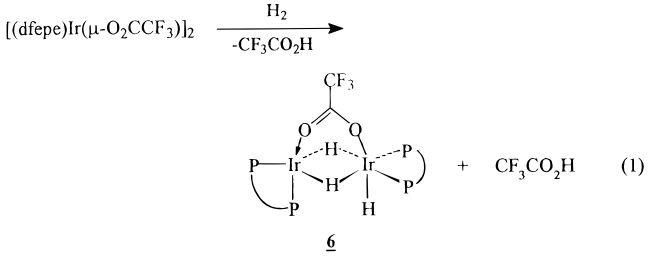

6

NMR data for **6** and the previously reported triflate analog (dfepe)$_2$Ir$_2$(μ-H)$_2$(H)(μ-O_3SCF_3)[6] are very similar and indicate that the two derivatives are isostructural. Surprisingly, the corresponding reaction between **5** and H_2 to give (dfepe)$_2$Ir$_2$(μ-H)$_2$(H)(μ-O_3SCF_3) is significantly slower: after 2 days, only a 20% conversion to the corresponding trihydride dimer is found. This difference in reactivity is contrary to expected bridging ligand labilities and indicates that an initial bridge dissociation is probably not rate-determining for hydrogenolysis. Instead, heterolysis of dihydrogen by **5** to form the stronger acid CF_3SO_3H may be rate-limiting.[18] The relative reactivities of **2** and **5** with benzene provide indirect support for this conclusion: unlike the CF_3CO_2-bridged dimer, which is unreactive at 80 °C, thermolysis of the triflate-bridged dimer **5** in benzene at 80 °C for 1 h quantitatively affords [(η^6-C_6H_6)Ir(dfepe)]$^+$OTf$^-$ (**7**) (eq 2). **7** may also be prepared from the thermolysis of **5**

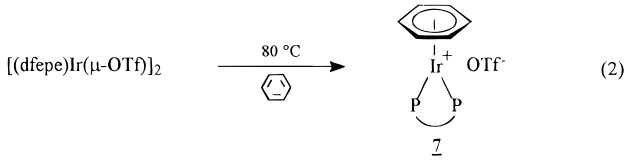

7

at 80 °C with excess cyclohexene in CH_2Cl_2. The formation of **7** from **5** and benzene indirectly reflects the enhanced lability anticipated for the triflate ligand.[19] The effect of added base on the heterolysis reactions of **2** and **5** would provide a more direct test for rate-limiting acid loss. Unfortunately, preliminary hydrogenation studies in the presence of Et_3N gave only uncharacterized product mixtures.

Scheme 3

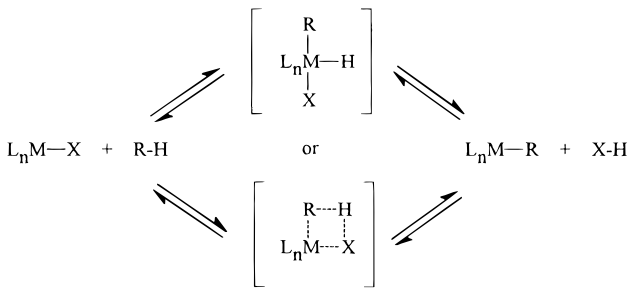

In addition to the reactions of **2** and **5** with H_2, the trifluoroacetate- and triflate-bridged iridium dimers also activate alkane C−H bonds. Thermolysis of **2** in neat cyclopentane at 150 °C cleanly afforded the previously reported cyclopentadienyl complex, CpIr(dfepe),[4] plus 1 equiv of trifluoroacetic acid per iridium center (eq 3). Again, under similar conditions the triflate-bridged analogue only yielded minor (*ca.* 20%) amounts of CpIr-(dfepe).

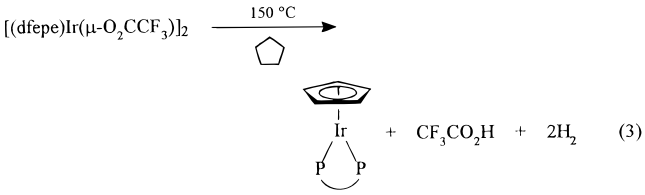

Summary

Hydrocarbon activation by group IX transition metals has primarily focused on electron-rich rhodium and iridium systems containing donor phosphine ancillary ligands. For the $(Me_3P)_2RhCl(L)$ systems studied extensively by Goldman and Sakakura, the reactive intermediate is believed to be the 3-coordinate 14-electron complex $(Me_3P)_2RhCl$. Access to this intermediate by thermal or photolytic ligand dissociation is a prerequisite step in this chemistry.[20] We have demonstrated that electron-poor iridium complexes containing (perfluoroalkyl)phosphine ligands are also capable of C−H activation under thermal conditions. Analogous (dfepe)Rh systems, however, do not exhibit similar reactivity.

Although the ease of bridge dissociation for [(dfepe)-Ir(μ-X)]$_2$ systems appears to be an important requirement in their chemistry, additional factors must contribute to the observed reactivity trends. In both hydrogenolysis and alkane dehydrogenation reactions, elimination of the corresponding acid HX is required by the overall stoichiometry of the reaction. *A priori*, heterolysis may proceed in either a concerted or stepwise fashion (Scheme 3). Undue mechanistic speculation is not warranted in the absence of quantitative data; however, the reversibility of HX loss subsequent to or concurrent with substrate addition is certainly reasonable, and the position of this equilibrium should therefore be sensitive to the acid strength of HX.

(17) (a) Fryzuk, M. D.; Gao, X.; Rettig, S. J. *J. Am. Chem. Soc.* **1995**, *117*, 3106. (b) Fryzuk, M. D.; Li, H.; McManus, N. T.; Paglia, P.; Rettig, S. J.; White, G. S. *Organometallics* **1992**, *11*, 2979. (c) Tulip, T. H.; Ibers, J. A. *J. Am. Chem. Soc.* **1979**, *101*, 4201. (d) Schoonover, M. W.; Baker, E. C.; Eisenberg, R. *J. Am. Chem. Soc.* **1979**, *101*, 1880. (e) Kaduk, J. A.; Poulos, A. T.; Ibers, J. A. *J. Organomet. Chem.* **1977**, *127*, 245.

(18) A reviewer has suggested that an intrinsic lower reactivity of **5** toward the oxidative addition of H−H or C−H bonds relative to **2** may also explain this reactivity trend.

(19) Complex **6** precipitates from benzene and thus does not directly measure solvolysis (and hence anion lability); however, any equilibrium formation of [(η^6-C_6H_6)Ir(dfepe)]$^+$$O_2CCF_3^-$ from thermolysis of **2** in benzene would also be driven by precipitation.

(20) Access to monomeric reactive intermediates via hydrogen addition to [$(R_3P)_2Rh(\mu$-Cl)]$_2$ has also been reported by Goldman.[2b]

Increased M−X lability is often cited as a criterion for metal-mediated heterolysis activity, but in light of the results described in this paper, it is apparent that the strength of the HX released in reactions with H_2 or R−H substrates may also play an important and potentially inhibitive role.

Experimental Section

General Procedures. All manipulations were conducted under an atmosphere of nitrogen using Schlenk, high-vacuum line and/or glovebox techniques. Dry, oxygen-free solvents were vacuum distilled prior to use. Cyclopentane for dehydrogenation experiments was prepared by hydrogenolysis of freshly cracked cyclopentadiene over 5% Pd/C, treated several times with H_2SO_4/HNO_3 to remove residual olefins, and dried with activated 4 Å molecular sieves. Elemental analyses were performed by Desert Analytics (Tucson, AZ). ^{19}F spectra were referenced to CF_3CO_2Et as an external standard (−75.32 ppm vs $CFCl_3$ with downfield chemical shifts taken to be positive). ^{31}P spectra were referenced to a 85% H_3PO_4 external standard. $[(cod)Ir(\mu\text{-}Cl)]_2$,[21] $[(cod)Rh(\mu\text{-}Cl)]_2$,[22] [(dfepe)Ir(cod)][$O_3SCF_3$],[6] and (dfepe)Ir($\eta^3$-$C_3H_5$)[15] were prepared by following literature procedures. The dfepe ligand was prepared as described previously.[23]

[(dfepe)Ir(cod)][(dfepe)Ir(O_2CCF_3)$_2$] (1). $[(cod)Ir(\mu\text{-}Cl)]_2$ (0.500 g, 0.744 mmol) and AgO_2CCF_3 (0.328 g, 1.49 mmol) were taken up in 50 mL of CH_2Cl_2 and stirred in the dark for 2 h. The solution was then filtered, and dfepe (0.968 g, 1.71 mmol) was added dropwise, during which time a red precipitate began to form. After the addition was complete the red crystalline solid was filtered off, washed twice with CH_2Cl_2, and dried under vacuum for 30 min, yielding 1.002 g (73%) of analytically pure **1**. Anal. Calcd for $C_{32}H_{20}F_{46}Ir_2O_4P_4$: C, 20.74; H, 1.08; F, 47.21. Found: C, 20.51; H, 0.82; F, 47.53. IR (cm^{-1}): 1730 m, 1703 s, 1417 m, 1295 s, 1227 sh, 1197 s, 1141 s, 1123 sh, 965 s, 959 sh, 747 m, 721 m, 664 w. UV−vis (KBr pellet, nm): 280, 348, 396, 500. UV−vis of [(dfepe)Ir(cod)]O_3SCF_3 (KBr pellet, nm): 252, 276, 384, 482, 576.

[(dfepe)Ir(μ-O_2CCF_3)]$_2$ (2). A suspension of 0.502 g of **1** in 50 mL of refluxing benzene dissolved over the course of 2 h to give a homogeneous yellow solution. Upon cooling of the sample to ambient temperature, canary yellow **2** precipitated in essentially quantitative yield (0.462 g, 98%). *Note*: When the thermolysis is carried out at higher concentrations, the labilization of cyclooctadiene from **1** is not complete. Anal. Calcd for $C_{24}H_8F_{46}Ir_2O_4P_4$: C, 16.48; H, 0.46. Found: C, 16.79; H, 0.78. IR (cm^{-1}): 1700 vs, 1297 vs, 1205 sh, 1132 s, 970 s. IR (CH_2Cl_2): 1674 cm^{-1} ($\nu(CO_2)_{asym}$). ^1H NMR (benzene-d_6, 269.7 MHz, 80 °C): δ 1.47 (m, 8H; PCH_2). ^{31}P NMR (benzene-d_6, 109.1 MHz, 80 °C): δ 65.10 (m). ^{19}F NMR (benzene-d_6, 376.05 MHz, 22 °C): δ −75.92 (s, O_2CCF_3), −80.15 (s, PCF_2CF_3), −113 to −115 (overlapping ABX multiplets, PCF_2CF_3).

[(dfepe)Rh(μ-O_2CCF_3)]$_2$ (3). $[(cod)Rh(\mu\text{-}Cl)]_2$ (0.501 g, 1.01 mmol) and AgO_2CCF_3 (0.500 g, 2.32 mmol) were taken up in 50 mL of CH_2Cl_2 and stirred in the dark at room temperature for 14 h. The solution was then filtered, and dfepe (1.308 g, 2.32 mmol) was added dropwise. The reaction mixture was stirred an additional 1 h, and the resulting orange precipitate was filtered off and washed twice with CH_2Cl_2. The yield of **3** after drying was 1.338 g (84%). Anal. Calcd for $C_{24}H_8F_{46}Rh_2O_4P_4$: C, 18.41; H, 0.51. Found: C, 18.20; H, 0.50. IR (cm^{-1}): 1705 s, 1668 sh, 1298 s, 1248 vs, 1205 sh, 1128 s, 1032 w, 965 s. IR (CH_2Cl_2): 1682 cm^{-1} ($\nu(CO_2)_{asym}$). ^1H NMR (acetone-d_6, 269.7 MHz, 22 °C): δ 2.68 (m, PCH_2). ^{31}P NMR (acetone-d_6, 109.1 MHz, 22 °C): δ 103.3 (dm, $^1J_{RhP}$ = 126 Hz). ^{19}F NMR (acetone-d_6, 376.05 MHz, 22 °C): δ −74.43 (s, O_2CCF_3), −78.48 (s, PCF_2CF_3), −111.14 (dd, PCF_2CF_3, $^2J_{FF}$ = 316 Hz, $^2J_{PF}$ = 49 Hz), −113.25 (dd, PCF_2CF_3, $^2J_{FF}$ = 319 Hz, $^2J_{PF}$ = 52 Hz).

(dfepe)Ir(η^3-C_3H_5)(H)O_3SCF_3 (4). A 30 μL (0.34 mmol) volume of triflic acid was added to a solution of (dfepe)Ir(η^3-C_3H_5) (0.250 g, 0.313 mmol) in 20 mL of CH_2Cl_2 at room temperature. The orange solution became colorless upon acid addition and was allowed to stir for 1 h. After the volatiles were removed under vacuum, the residue was triturated with several mL of ether, and the resulting white microcrystalline precipitate was collected and washed twice with ether; the isolated yield of **4** was 0.261 g (88%). Anal. Calcd for $C_{14}H_{10}IrF_{23}O_3P_2S$: C, 17.70; H, 1.05. Found: C, 17.29; H, 0.89. IR (cm^{-1}): 1409 w, 1373 m, 1313 s, 1224 s, 1214 s, 1178 m, 1163 m, 1134 s, 1110 s, 1027 s, 976 s. ^1H NMR (CD_2Cl_2, 399.65 MHz, 20 °C): δ −30.41 (t, $^2J_{PH}$ = 15 Hz, 1H; IrH), 2.63 (m, 2H; PCH_2), 2.95 (m, 2H; PCH_2), 3.79 (m, 2H; H_{anti}), 4.62 (m, 2H; H_{syn}), 5.30 (m, 1H; $H_{central}$). ^{31}P NMR (CD_2Cl_2, 161.9 MHz, 20 °C): δ 69.5 (m). ^{19}F NMR (CD_2Cl_2, 376.05 MHz, 20 °C): δ −77.17, −77.50 (s, PCF_2CF_3), −78.71 (s, O_3SCF_3), −104 to −106, −109 to −112 (overlapping ABX multiplets, PCF_2CF_3).

[(dfepe)Ir(μ-O_3SCF_3)]$_2$ (5). A slurry of **4** (0.502 g, 0.628 mmol) in 30 mL of heptane was heated to reflux for 1 day. The volatiles were removed under vacuum, and the residue was triturated with ether. The resulting light yellow solid was collected by filtration and washed several times with ether and dried under vacuum. The isolated yield of **5** was 0.498 g (87%). Anal. Calcd for $C_{22}H_8F_{46}O_6Ir_2P_4S_2$: C, 14.56; H, 0.44. Found: C, 14.49; H, 0.44. IR (cm^{-1}): 1324 sh, 1298 s, 1218 vs, 1174 s, 1138 s, 1063 m, 1019 s, 972 s, 874 w, 809 w, 750 m. ^1H NMR (acetone-d_6, 399.65 MHz, 27 °C): δ 2.61 (m, PCH_2). ^{31}P NMR (acetone-d_6, 161.7 MHz, 27 °C): δ 67.4 (m). ^{19}F NMR (acetone-d_6, 376.05 MHz, 27 °C): δ −77.22 (s, O_3SCF_3), −77.86 (s, PCF_2CF_3), −111 to −114 (overlapping ABX multiplets, PCF_2CF_3).

(dfepe)$_2$Ir$_2$(H)(μ-H)$_2$(μ-O_2CCF_3) (6). A Carius tube fitted with a 4 mm Teflon vacuum valve (Kontes) was charged with 0.125 g of **2** (0.072 mmol), 20 mL of benzene, and 1 atm of H_2 and heated to 80 °C for 2 h. After cooling, the solution was transferred to a swivel filtration assembly and the solvent was removed. The residue was extracted with acetone, and the filtrate was reduced to ca. 2 mL and cooled to −78 °C. Cold filtration of the resulting precipitate afforded 0.098 g (83%) of bright yellow **6**. Anal. Calcd for $C_{20}H_{11}F_{43}Ir_2O_2P_4$: C, 16.18; H, 0.67. Found: C, 16.18; H, 0.67. IR (cm^{-1}): 1659 m, 1634 w, 1335 m, 1308 s, 1224 s, 1142 s, 1118 s, 1026 m, 967 s. ^1H NMR (benzene-d_6, 269.7 MHz, 22 °C): δ 2.01 (m, 2H; PCH_2), 1.62 (m, 2H; PCH_2), −6.01 (dd, $^2J_{PH}$(cis) = 43 Hz, $^2J_{PH}$(trans) = 116 Hz, 2H; Ir(μ-H)), −24.50 (t, $^2J_{PH}$ = 12 Hz, 1H; Ir(H)). ^{31}P NMR (acetone-d_6, 109.1 MHz, 22 °C): δ 63.4, 80.1, 88.1 (multiplets). ^{19}F NMR (acetone-d_6, 376.05 MHz, 22 °C): δ −73.33 (s, O_2CCF_3), −76.36, −76.95, −77.11, −78.85 (s, PCF_2CF_3), −107.6 to −114.9 (overlapping ABX multiplets, PCF_2CF_3).

[(η^6-C_6H_6)Ir(dfepe)][O_3SCF_3] (7). A Carius tube was charged with 0.500 g (0.493 mmol) of [(dfepe)Ir(cod)][O_3SCF_3], 35 mL of CH_2Cl_2, and 1 mL of cyclohexene and was heated to 80 °C for 2 h. Initially dark red, the solution turned bright yellow during the course of the thermolysis. The cooled solution was filtered, the volume was reduced to a *ca*. 2 mL, and 5 mL of petroleum ether was added. The resulting light yellow precipitate was washed twice with petroleum ether and dried under vacuum. The yield of **7** was 0.350 g (77%). Anal. Calcd for $C_{17}H_{10}IrF_{43}O_3P_2S$: C, 20.71; H, 1.01. Found: C, 20.62; H, 0.91. IR (cm^{-1}): 3095 w, 1298 s, 1288 s, 1230 vs, 1137 s, 1031 s, 967 s, 812 m, 752 m, 722 m. ^1H NMR (acetone-d_6, 269.7 MHz, 20 °C): δ 7.42 (s, 6H, C_6H_6), 3.03 (m, 4H, PCH_2). ^{31}P NMR (acetone-d_6, 109.1 MHz, 20 °C): δ 74.3 (m). ^{19}F NMR

(21) Herde, J. L.; Lambert, J. C.; Senoff, C. V. *Inorg. Synth.* **1974**, *15*, 18.
(22) Giordano, G.; Crabtree, R. H. *Inorg. Synth.* **1979**, *19*, 218.
(23) Ernst, M. F.; Roddick. D. M. *Inorg. Chem.* **1989**, *28*, 1624.

(acetone-d_6, 376.05 MHz, 20 °C): δ −76.89 (s, PCF_2CF_3), −78.41 (s, O_3SCF_3), −110.55 (dd, $^2J_{FF}$ = 316 Hz, $^2J_{PF}$ = 64 Hz; PCF_2CF_3), −113.70 (dd, $^2J_{FF}$ = 320 Hz, $^2J_{PF}$ = 79 Hz; PCF_2CF_3).

Thermolysis Reactions of 2 and 5. In a typical experiment, a 5 mm NMR tube with a soft glass extension was charged with 5−10 mg of iridium compound and 0.4 mL of solvent. For hydrogenation reactions 570 Torr of H_2 was admitted and the tube was cooled to −195 °C and then sealed off with a torch. For cyclopentane, benzene, or cyclohexene thermolyses the NMR tubes were sealed under nitrogen. Thermolyses were carried out in a Hewlett Packard 5890 GC oven.

Crystal Structure of [(dfepe)Ir(μ-O_2CCF_3)]$_2$ (2). X-ray data were collected on a Siemens R3m/V automated diffractometer system. The radiation used was Mo Kα monochromatized by a highly-ordered graphite crystal. The parameters used during the data collection are summarized in Table 1. All computations used the SHELXTL/IRIS (version 4.2) program library (Siemens Corp., Madison, WI). A suitable crystal of **2** was grown from a saturated benzene solution. Monoclinic unit cell dimensions were derived from a least-squares fit of 50 random reflections (18° < 2θ < 28°). Data were collected using the 2θ/θ scan technique with a variable scan rate of 4.0−30.0 deg/min. Three standard reflections monitored after every 100 data collected showed no systematic variation. $P2_1/n$ space group symmetry was deduced from a statistical analysis of all collected data. Data were corrected for absorption using an empirical ellipsoidal model based on 360° ψ-scans for 12 reflections with 10°< 2θ < 35°.

The molecular structure of **2** was solved using the SHELXTL direct methods program; all non-hydrogen atoms were located on a series of difference Fourier maps. The iridium, phosphorus, and trifluoroacetate atoms were refined anisotropically. All other non-hydrogen atoms (20 carbon, 40 fluorine) were refined isotropically due to data/parameter limitations. Chelate backbone hydrogen atom positions were added in ideal calculated positions with d(C−H) = 0.96 Å and with fixed isotropic thermal parameters set at approximately 1.3 times the value of the attached carbon atom. Full-matrix least-squares refinement on F ($I > 2\sigma(I)$) for 3982 data gave an R value of 6.81%. The final difference Fourier map showed residual peaks of 2.15 and −1.75 e/Å^3 in the region surrounding the platinum centers due to uncompensated absorption.

Crystal Structure of (dfepe)Ir(η^3-C_3H_5)(H)O_3SCF_3 (4). X-ray data were collected and computations were performed as described above. The parameters used during the data collection are summarized in Table 1. A suitable crystal of **4** was grown from dichloromethane. Orthorhombic unit cell dimensions were derived from a least-squares fit of 50 random reflections (18° < 2θ < 29°). Data were collected using the Wyckoff scan technique with a variable scan rate of 4.0−30.0 deg/min. Two standard reflections monitored after every 100 data collected showed no systematic variation. $P2_12_12_1$ space group symmetry deduced from a statistical analysis of all collected data was confirmed by subsequent refinements. Data were corrected for absorption using the empirical program XABS2.[24]

The molecular structure of **4** was solved using the SHELXTL direct methods program; all non-hydrogen atoms were located on a series of difference Fourier maps. Chelate backbone hydrogen atom positions were modeled as described above. All non-hydrogen atoms were refined anisotropically. The hydride ligand was not located and was excluded from the final refinement model. A Flack parameter test on the full refined data set indicated that the opposite absolute structure was correct; the coordinates for all atoms were therefore inverted. Full-matrix least-squares refinement on F gave an R value of 5.29% (R_w = 5.81%) for 2645 data with $I > 2\sigma(I)$. The final difference Fourier map showed residual peaks of 2.61 and −2.00 e/Å^3 associated with the iridium center.

Acknowledgment. This work has been supported by the National Science Foundation (Grant CHE-9310550). Johnson Matthey is gratefully acknowledged for a generous loan of iridium and rhodium chlorides.

Supporting Information Available: UV−vis spectra for **1** and [(dfepe)Ir(cod)]O_3SCF_3 and tables of final positional parameters and isotropic and anisotropic displacement parameters for all atoms and complete bond lengths and angles for **2** and **4** (19 pages). Ordering information is given on any current masthead page.

OM9602163

(24) Parkin, S.; Moezzi, B.; Hope H. *J. Appl. Crystallogr.* **1995**, *28*, 53.